Polymer Chemistry

Mechanical Properties and Molecular Adhesion Exhibited by Inorganic–Organic Composite Elastomers

Journal:	*Polymer Chemistry*
Manuscript ID	PY-ART-08-2024-000879.R1
Article Type:	Paper
Date Submitted by the Author:	21-Sep-2024

Complete List of Authors:	Yamashita, Naoki; Graduate School of Science, Osaka University, Department of Macromolecular Science Ikura, Ryohei; Graduate School of Science, Osaka University, Department of Macromolecular Science Yamaoka, Kenji; Osaka University, Graduate School of Science, Department of Macromolecular Science Kato, Nobu; Shinetsu Kagaku Kogyo Kabushiki Kaisha Kamei, Masanao; Shin-etsu Chemical Co Ltd Ogura, Kentaro; Shinetsu Kagaku Kogyo Kabushiki Kaisha Igarashi, Minoru; Shinetsu Kagaku Kogyo Kabushiki Kaisha Nakagawa, Hideo; Shin-etsu Chemical Co Ltd Takashima, Yoshinori; Graduate School of Science, Osaka University, Department of Macromolecular Science; Institute for Advanced Co-Creation Studies,

ARTICLE

Mechanical Properties and Molecular Adhesion Exhibited by Inorganic–Organic Composite Elastomers

Received 00th January 20xx,
Accepted 00th January 20xx

DOI: 10.1039/x0xx00000x

Naoki Yamashita,[a] Ryohei Ikura,[ab] Kenji Yamaoka,[ab] Nobu Kato,[c] Masanao Kamei,[c] Kentaro Ogura,[c] Minoru Igarashi,[c] Hideo Nakagawa,[d] and Yoshinori Takashima*[abe]

Polydimethylsiloxane (PDMS)-based organic–inorganic composites have attracted considerable attention due to PDMS's unique features, such as transparency, softness, biocompatibility, chemical stability, heat resistance, and insulation. To extend the lifespans of organic–inorganic composites, high mixability and self-healing properties are needed. Herein, organic–inorganic composite elastomers with reversible cross-links featuring cyclodextrin (CD)-modified PDMS (PDMS-CD) and adamantane (Ad)-modified poly(alkyl acrylate) were prepared to achieve high mixability and molecular adhesion properties. PDMS-CD/P(EA-Ad) (*x*) was obtained by the solution polymerization of ethyl acrylate (EA) and an adamantane monomer (AdAAm) in the presence of PDMS-CD. *x* is the molar ratio of Ad to βCD. The excess Ad units in PDMS-CD/P(EA-Ad) (5) result in high stretchability and effective self-healing properties based on molecular adhesion. The stress relaxation tests show that excess amounts of Ad units improve the reformation and exchange characteristics of reversible cross-links. A structural study using small-angle X-ray scattering (SAXS) reveals that many Ad units improve the mixability of PDMS and acrylate polymers to effectively reform reversible cross-links and increase the healing efficiency.

Introduction

Research on the compositing of multiple polymers has been widely performed to achieve the strength of each polymer, simultaneously[1–5]. In particular, polydimethylsiloxane (PDMS)-based organic–inorganic composites have attracted considerable attention due to PDMS's unique features, such as transparency[6,7], softness[8,9], biocompatibility[10,11], chemical stability[12], heat resistance[13,14], and insulation[15]. These properties are expected to allow wide application in industrial[16,17], medical[18,19], electrical[20,21], and academic fields. However, there are two challenges associated with these PDMS-based composites. One challenge is the low mixability of PDMS and organic polymers due to the large differences between their solubility parameters[22–24]; this difficulty in mixing leads to the brittleness and turbidity of the composites. Many researchers have performed reactive blending to overcome this issue[25–30]. This approach provides high mixability through the use of chemical cross-links connecting PDMS and organic polymers. Interpenetrating approaches[31–33] also can improve mixability to create colorless and tough organic–inorganic composites[34]. However, these composites are not suitable for repeated use due to the breakage of chemical cross-links through stress concentrations during deformation.

The other challenge is the limitation of the lifetimes of these materials due to their irreversible breakage, while the aforementioned applications require long-term use to reduce costs and invasiveness by reoperation for replacement of implanted medical devices[35]. There are two approaches for improving the lifetimes by self-healing properties: (i) restriction of breakage by self-restoration[36–41] and (ii) repair of damage by molecular adhesion[42–58]. Self-restoring properties regain their original shapes and mechanical properties of tough elastic materials after deformation. The driving force in self-restoration is entropic elasticity. Molecular adhesion properties repair the wounds. The driving force in molecular adhesion is the repeated cleavage and reformation of reversible cross-links consisting of noncovalent bonds.

Previously, we prepared PDMS elastomers with reversible cross-links consisting of inclusion complexes of cyclodextrin (CD) and adamantane (Ad), which exhibited molecular adhesion properties[59]. We also prepared tough PDMS-based elastomers with movable cross-links consisting of PDMS polymer penetrating CD cavities[60]. Moreover, improvements in mixability were achieved by connecting PDMS and organic polymers with movable cross-links [61]. However, this work also revealed that hydrogen bonds in intradomains could reduce compatibility.

Herein, we hypothesized that reversible cross-links between PDMS and organic polymers would improve the mixability and

[a] Department of Macromolecular Science, Graduate School of Science, Osaka University, 1-1 Machikaneyamacho, Toyonaka, Osaka 560-0043, Japan
[b] Forefront Research Center, Graduate School of Science, Osaka University,1-1 Machikaneyamacho, Toyonaka, Osaka 560-0043, Japan
[c] Shin-Estu Chemical Co., Ltd., Silicone-Electronics Materials Research Center, 1-10, Hitomi, Matsuida-machi, Annaka-shi, Gunma 379-0224, Japan
[d] Shin-Etsu Chemical Co., Ltd., 4-1 Marunouchi, 1-chome, Chiyoda-ku, Tokyo 100-0005, Japan
[e] Innovative Catalysis Science Division, Institute for Open and Transdisciplinary Research Initiatives, Osaka University, 1-1 Yamadaoka, Suita, Osaka 565-0871, Japan
†Electronic Supplementary Information (ESI) available. See
DOI: 10.1039/x0xx00000x

self-healing properties. We prepared organic–inorganic composite elastomers with βCD-modified PDMS with Ad-modified acrylate polymers (**Figure 1**). Inclusion complexes between βCD and Ad units are expected to form reversible cross-links connecting PDMS and organic polymers without intradomain interactions. The introduction of reversible cross-links improved the mixability of organic and inorganic polymers and provided molecular adhesion properties. Furthermore, we investigated the effect of the molar ratio of Ad to βCD on the mechanical, stress relaxation, and molecular adhesion properties.

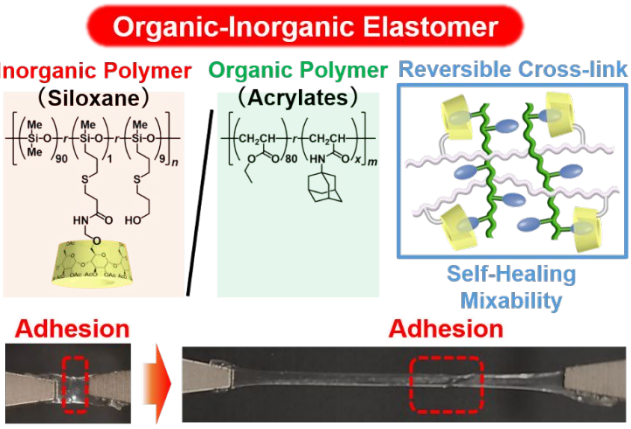

Figure 1. Schematic of organic–inorganic composite elastomers (PDMS-CD/P(EA-Ad) (*x*)) obtained by introducing reversible cross-links.

Results and discussion

Preparation of organic–inorganic composite elastomers

The organic–inorganic composite elastomers were fabricated by one-pot reactions with two steps (details of the reaction procedures and contents of the reagents are shown in **Schemes S1 and S2 and Table S1**). The first step is the preparation of cyclodextrin-modified PDMS (PDMS-CD) via a thiol–ene reaction with thiol-modified PDMS (PDMS-SH), triacetylated 6-acrylamido methylether-β-cyclodextrin (TAcβCDAAmMe), and allyl alcohol. Allyl alcohol prevents the unintended formation of chemical cross-links from residual SH groups. The thiol-ene reaction is carried out in ethyl acetate with a photoradical initiator (2-hydroxy-2-methylpropiophenone; IRGACURE 1173). The second step is the compositing of organic and inorganic polymers by the polymerization of adamantane-modified poly(ethyl acrylate) (PEA) in the presence of PDMS-CD. The main chain monomer (EA), guest monomer (*N*-(1-adamantyl)acrylamide; AdAAm), and photoradical initiator (phenylbis(2,4,6-trimethylbenzoyl)phosphine oxide; BAPO) were added to the obtained solution of PDMS-CD. Then, photoradical polymerizations were carried out. After removing the solution, the obtained organic–inorganic composite elastomers are abbreviated as PDMS-CD/P(EA-Ad) (*x*), where *x* is the molar ratio of Ad to βCD (**Figure 2a**). As negative control samples, PDMS-CD/PEA without Ad units, PDMS/P(EA-Ad) (5) without CD units, and PDMS/PEA without CD or Ad units were obtained in a similar manner (**Schemes S3–S5**). These organic–inorganic composite elastomers are transparent and show high mixability (**Figure 2b**). The chemical structures of the obtained materials were characterized by ^{1}H nuclear magnetic resonance (NMR) and Fourier transform infrared (FT-IR) spectroscopy (**Figures S1–S12**). The molecular weight of the PDMS-CD specimen was characterized by gel permeation chromatography (GPC) (**Figure S13**). The complexation between βCD and Ad was confirmed by 2D nuclear Overhauser effect spectroscopy (NOESY) NMR (**Figure S14**).

Investigation of the effects of reversible cross-link exchange on the mechanical properties of organic–inorganic composite elastomers

The mechanical properties of the organic–inorganic composite elastomers were investigated by tensile tests (tensile rate: 1 mm/s). **Figure 3a** shows the stress–strain curves of PDMS-CD/P(EA-Ad) (5), PDMS-CD/PEA, PDMS/P(EA-Ad) (5), and PDMS/PEA. PDMS-CD/P(EA-Ad) (5) has the highest fracture stress, and it supports the formation of reversible cross-links. PDMS-CD/P(EA-Ad) (5) has the highest fracture strain. While the stress–strain curve of PDMS/PEA shows a monotonic increase in stress, that of PDMS-CD/P(EA-Ad) (5) shows an S-shaped curve with a wide range (ε = 200–800%) and small slopes. These results suggest that effective stress relaxation by host–guest complexes increases the fracture strain of PDMS-CD/P(EA-Ad) (5). **Figure 3b** shows plots of the relationship between the toughness and Young's modulus. The toughness and Young's modulus were calculated from the integral and the initial slope of the stress–strain curve, respectively. PDMS-CD/P(EA-Ad) (5) show almost the same Young's modulus as PDMS-CD/PEA, and smaller than PDMS/PEA. The toughness of PDMS-CD/P(EA-Ad) (5) is 24 times greater than that of PDMS/PEA and 2.4 times greater than that of PDMS-CD/PEA. These results indicate that host–guest complexation between CD and Ad contributes to increased toughness. Notably, the higher toughness of PDMS-CD/PEA than that of PDMS/PEA is derived from the presence of movable cross-links consisting of PEA chains penetrating the CD units.

To obtain insight into the effects of host–guest complexation on the mechanical properties, we investigated the relationships between the mechanical properties and the contents of guest units in the organic–inorganic composite elastomers. **Figures 3c and 3d** show the stress–strain curves and relationships between the toughness and Young's modulus values of PDMS-CD/PEA and PDMS-CD/P(EA-Ad) (*x*) (*x* = 1, 2, and 5). While these elastomers exhibit similar fracture stress and Young's modulus values, their toughness and fracture strain values increase with the increase in the number of Ad units. These results indicate that the addition of many Ad units helps in the achievement of high toughness via reversible cross-link exchange. The cyclic tensile test of PDMS-CD/P(EA-Ad) (5) shows effective recovery of the mechanical properties at middle strain region (**Figure S15**). These results support that the S-shaped curve with a wide range is attributed to the stress-relaxation by exchange of reversible cross-links.

Evaluation of molecular adhesion by re-adhesion tests

To investigate the relationship between the molecular adhesion properties and the contents of guest units in the

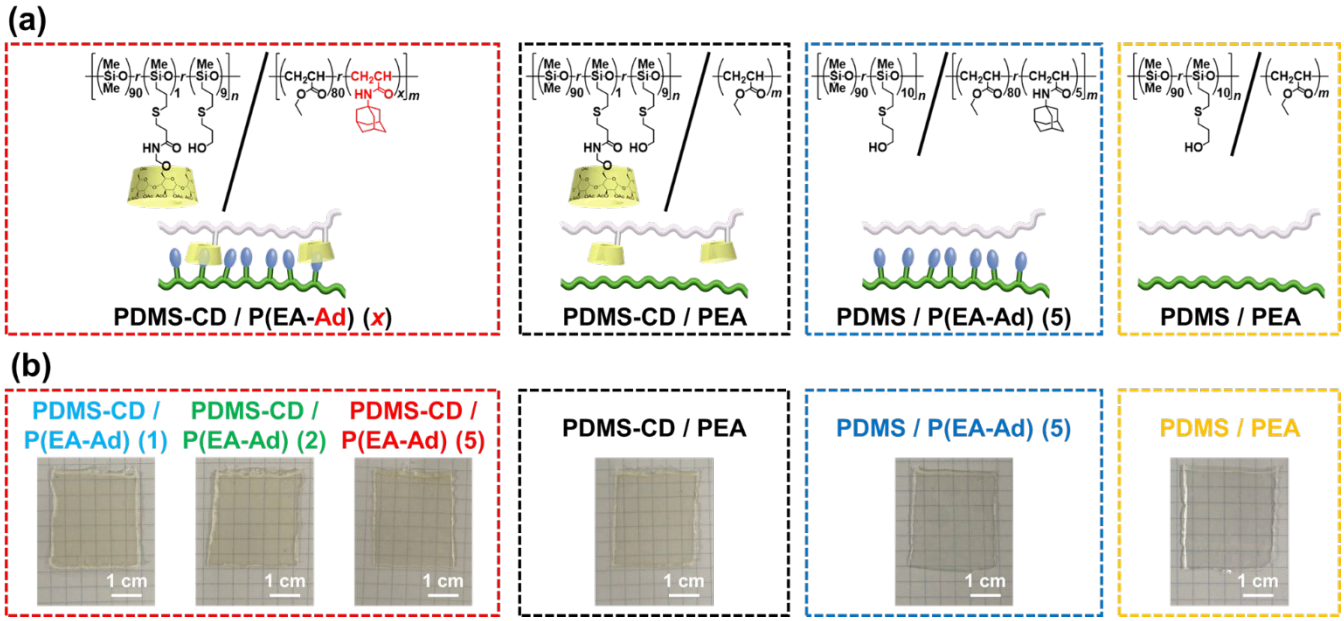

Figure 2. (a) Chemical structures and **(b)** photographs of PDMS-CD/P(EA-Ad) (*x*), PDMS-CD/PEA, PDMS/P(EA-Ad) (5), and PDMS/PEA. *x* is the molar ratio of Ad to βCD.

organic–inorganic composite elastomers, a re-adhesion test was conducted. PDMS-CD/PEA and PDMS-CD/P(EA-Ad) (*x*) (*x* = 1, 2, and 5) were cut into two pieces and reattached. These elastomers exhibit surface-selective adhesion derived from the reformation of host–guest complexes (**Figure 4a and Movie S1**). The reattached pieces were left for 24 hours at room temperature or for 12 hours at 70 °C, after which tensile tests were carried out again (**Figure 4b**). The healed sample of PDMS-CD/P(EA-Ad) (5) shows greater stretchability than that of PDMS-CD/PEA (**Figures 4c and d and Movie S2**). **Figure 4e** shows the stress–strain curves of PDMS-CD/PEA and PDMS-CD/P(EA-Ad) (*x*) before cutting (original) and after adhering them for 12 hours at 70 °C (re-adhered). **Figure 4f** shows plots of their toughness and Young's modulus values. The healing ratio is determined with the following equation:

$$\text{Healing ratio} = \frac{\text{Toughness of re- adhered sample}}{\text{Toughness of original sample}} \times (1)$$

Figure 4g shows the healing ratios of PDMS-CD/PEA and PDMS-CD/P(EA-Ad) (*x*). All the samples have higher healing ratios at 70 °C than at room temperature. As a result, PDMS-CD/PEA also exhibits re-adhesion. This phenomenon is attributed to the reformation of movable cross-links when the cut pieces are reattached. PEA chains in PDMS-CD/PEA do not have bulky stoppers that CD units cannot pass over, allowing PEA chains to penetrate CD units to reform movable cross-links[62]. PDMS-CD/P(EA-Ad) (1) has a lower healing ratio than PDMS-CD/PEA. This result suggests the formation of reversible and movable cross-links. The movable cross-links in PDMS-CD/P(EA-Ad) (1) have structures interlocked by Ad units that act as bulky stoppers inhibiting the reformation of movable cross-links to decrease the healing ratio. In swelling tests of PDMS-CD/PEA and PDMS-CD/P(EA-Ad) (*x*) (**Figure S16**), the smallest swelling ratio of PDMS-CD/P(EA-Ad) (1) supports the interlocked structures of movable cross-links. The healing ratios of PDMS-CD/P(EA-Ad) (*x*) increase with increasing *x*, indicating that excess amounts of Ad units facilitate the reformation of reversible cross-links. Considering the high swelling ratios of PDMS-CD/P(EA-Ad) (2) and PDMS-CD/P(EA-Ad) (5) shown in **Figure S16**, excess amounts of the Ad monomer suppress the unintended formation of movable cross-links and interlocked structures. These effects allow high healing efficiency by excess Ad units in PDMS-CD/P(EA-Ad) (5).

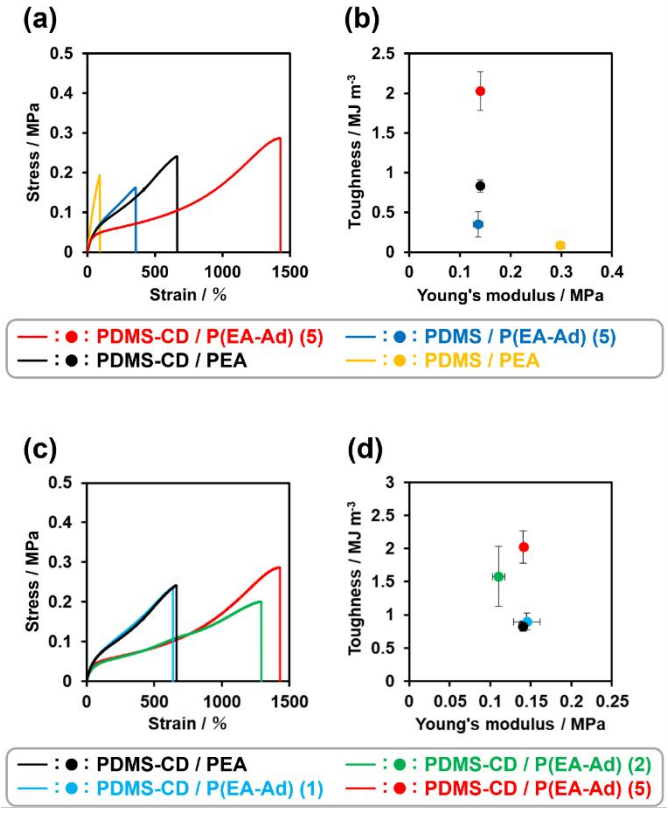

Figure 3. (a) Stress–strain curves and **(b)** plots of the toughness and Young's modulus values of PDMS-CD/P(EA-Ad) (5), PDMS-CD/PEA, PDMS/P(EA-Ad) (5), and PDMS/PEA. **(c)** Stress–strain curves and **(d)** plots of the toughness and Young's modulus values of PDMS-CD/PEA and PDMS-CD/P(EA-Ad) (*x*) (*x* = 1, 2, and 5).

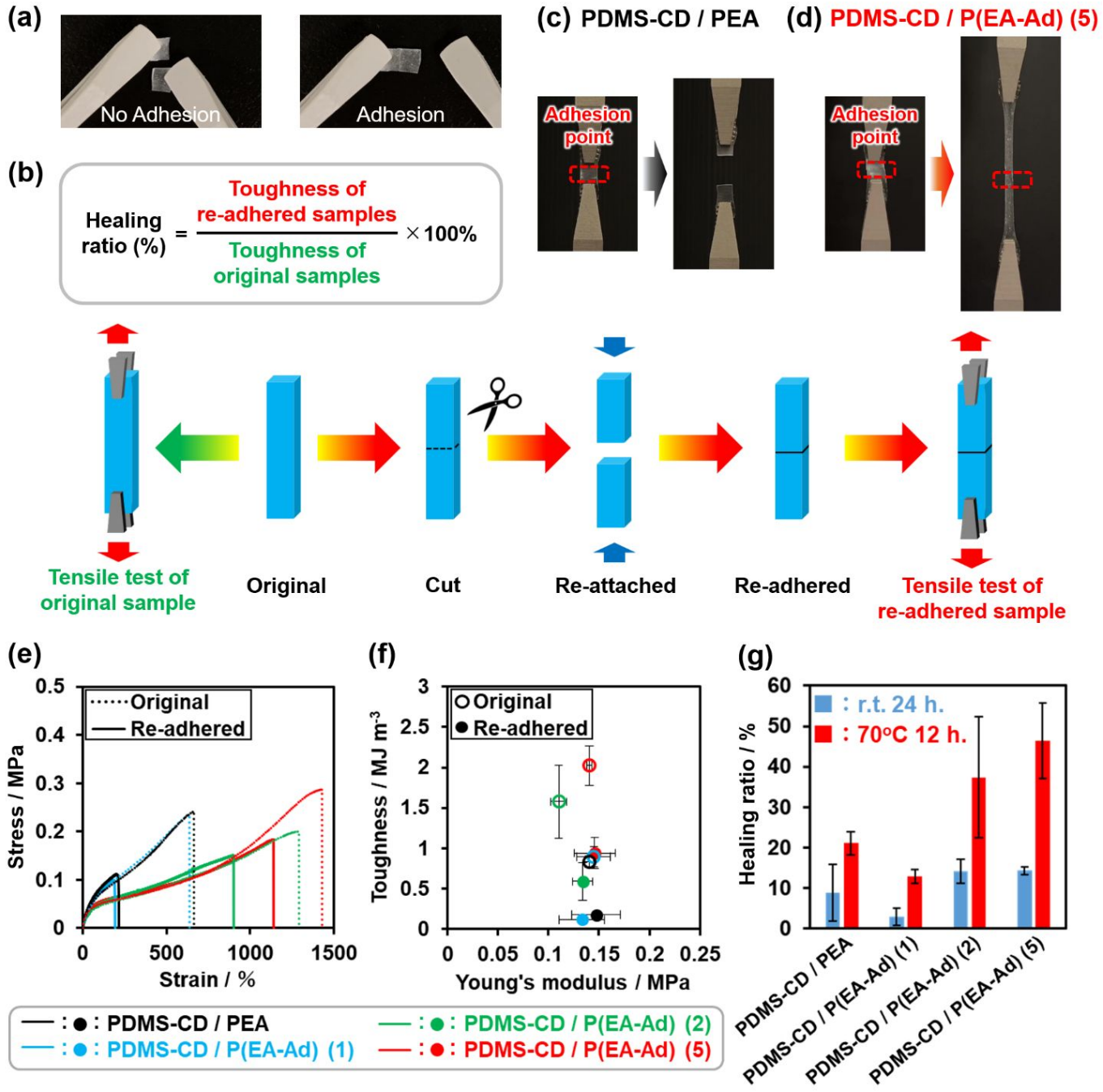

Figure 4. (a) Photographs of PDMS-CD/P(EA-Ad) (5) exhibiting surface-selective adhesion captured from **Movie S1**. **(b)** Experimental procedure of the re-adhesion test. Images of the re-adhesion test for **(c)** PDMS-CD/PEA and **(d)** PDMS-CD/P(EA-Ad) (5). **(e)** Stress–strain curves and **(f)** plots of the toughness and Young's modulus values of the original and re-adhered samples at 70 °C for PDMS-CD/PEA and PDMS-CD/P(EA-Ad) (*x*) (*x* = 1, 2, and 5) specimens healed for 12 hours. **(g)** Healing ratios of PDMS-CD/PEA and PDMS-CD/P(EA-Ad) (*x*).

Evaluation of the reformation and exchange of reversible cross-links by stress relaxation tests

To investigate the relationships between the reformation and exchange properties of reversible cross-links and the contents of guest units in the organic–inorganic composite elastomers, a stress relaxation test was conducted. PDMS-CD/PEA and PDMS-CD/P(EA-Ad) (*x*) (*x* = 1, 2, and 5) were stretched to an elongation of 100%. Then, the strain was held constant, and the stress was recorded for 1000 seconds (**Figure 5a**). The stress relaxation behavior is plotted by normalizing the stress (**Figure 5b**). To quantitatively evaluate the stress relaxation behavior, curve fitting was carried out on the obtained normalized stress–time curve using the Kohlrausch–Williams–Watts (KWW) equation shown below (**Figure S17**).

$$\sigma = \sigma_r \exp\left\{-\left(\frac{t}{\tau}\right)^{\beta}\right\} + \sigma_\infty (2)$$

where σ_r is the relaxable stress, σ_∞ is the residual stress, τ is the time constant, and β is the stretching exponent. The fitting

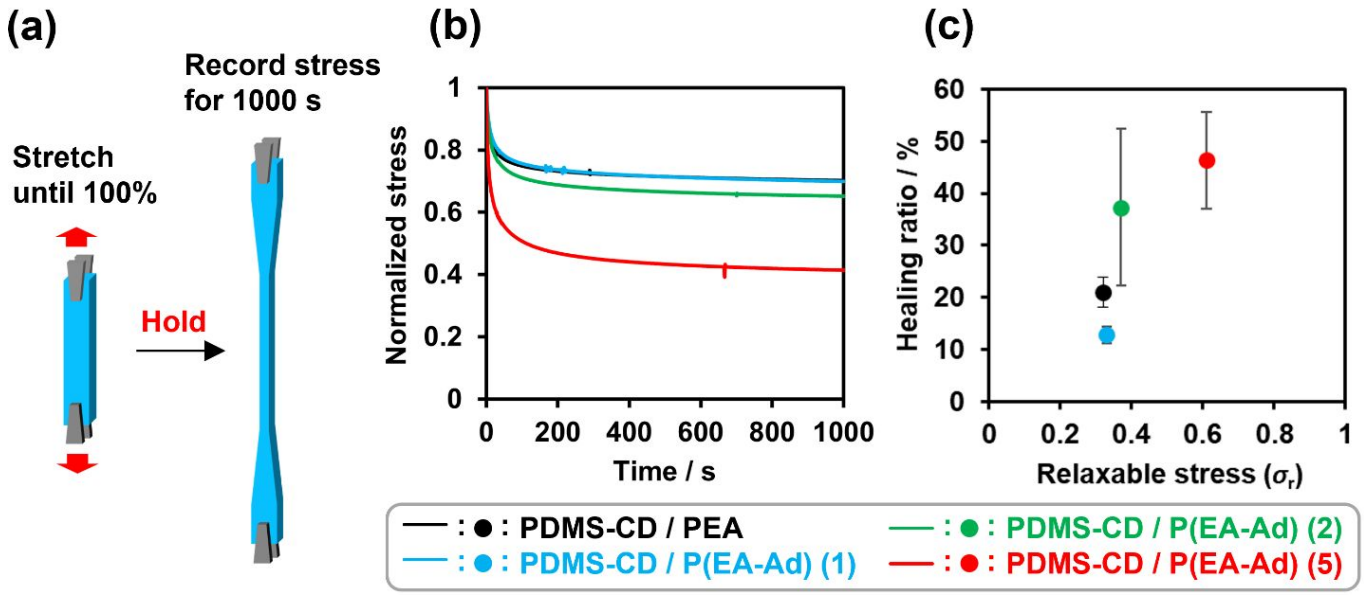

Figure 5. (a) Experimental procedure for the stress relaxation test. **(b)** Normalized stress relaxation curves and **(c)** plots of the relaxable stress (σ_r) and healing ratio for PDMS-CD/PEA and PDMS-CD/P(EA-Ad) (x) (x = 1, 2, and 5).

parameters of the KWW model are listed in **Table 1 and Table S2**. As a result, the σ_r values increase with increasing x, indicating that the excess Ad units result in effective stress dispersion based on reversible crosslink reformation and exchange. In the tensile test with slow tensile rate (0.1 mm/s) (**Figure S18**), PDMS-CD/PEA and PDMS-CD/P(EA-Ad) (x) (x = 1, 2, and 5) show the similar dependency of mechanical properties with tensile rate. Similar time constant τ contributes to the rate-dependency. **Figure 5c** shows that the healing ratio increases with increasing σ_r. These results supported that the excess Ad units in PDMS-CD/P(EA-Ad) (5) facilitate the reformation and exchange of reversible cross-links to achieve the highest healing efficiency.

Table 1. Fitting parameters obtained using the KWW models.

	Relaxable component			Residual component
	σ_r	τ / s	β	σ_∞
PDMS-CD/PEA	0.32	16	0.33	0.68
PDMS-CD/P(EA-Ad) (1)	0.33	17	0.33	0.67
PDMS-CD/P(EA-Ad) (2)	0.37	21	0.37	0.63
PDMS-CD/P(EA-Ad) (5)	0.61	19	0.36	0.39

Investigation of the mixability by structural analysis using SAXS

Small-angle X-ray scattering (SAXS) measurements were conducted to evaluate the phase-separated structures of PDMS-CD/P(EA-Ad) (5), PDMS-CD/PEA, PDMS/P(EA-Ad) (5), and PDMS/PEA (**Figure 6a**). The SAXS profiles of all the samples show significant peaks at approximately q = 0.4 nm^{-1} that correspond to the correlations between the PDMS phases and the PEA phases. The domain spacing (d) of the phase-separated structure of each composite elastomer was estimated with the following equation:

$$d = \frac{2\pi}{q^*} (3)$$

where q^* is the q value at the peak top in the SAXS region. The d values are listed in **Table 2**. All the elastomers have d values that are smaller than the wavelength of visible light, leading to their high transparency levels. PDMS-CD/P(EA-Ad) (5) has a smaller d value than the elastomers without βCD and Ad. Reversible cross-links improve the mixability of PDMS and PEA. The severe phase separation observed in PDMS/PEA was responsible for the high Young's modulus derived from larger PEA domain with a Young's modulus of about 0.7 MPa[41]. PDMS/P(EA-Ad) (5) has a smaller d value than PDMS/PEA because adamantane with low polarity improve the mixability of PDMS and P(EA-Ad). The decreased polarity of PEA-Ad reduces the differences of solubility parameters with PDMS-CD having lower polarity.

To effectively understand the effects of reversible cross-links on phase-separated structures, we investigated the relationship between the d values and the number of guest units in the organic–inorganic composite elastomers. **Figure 6b and Table 2** show the SAXS profiles and d values of PDMS-CD/PEA and PDMS-CD/P(EA-Ad) (x) (x = 1, 2, and 5). The d values decrease with the increase in the number of Ad units. The presence of many Ad units contributes to the improvement in the mixability. **Figure 6c** shows the relationship between d and the healing ratio. PDMS-CD/P(EA-Ad) (5) exhibits an improved mixability of PDMS and PEA to allow the effective reformation of reversible cross-links and an increase in the healing efficiency.

Conclusions

We prepared organic–inorganic composite elastomers using reversible cross-links consisting of βCD and Ad. PDMS-CD/P(EA-

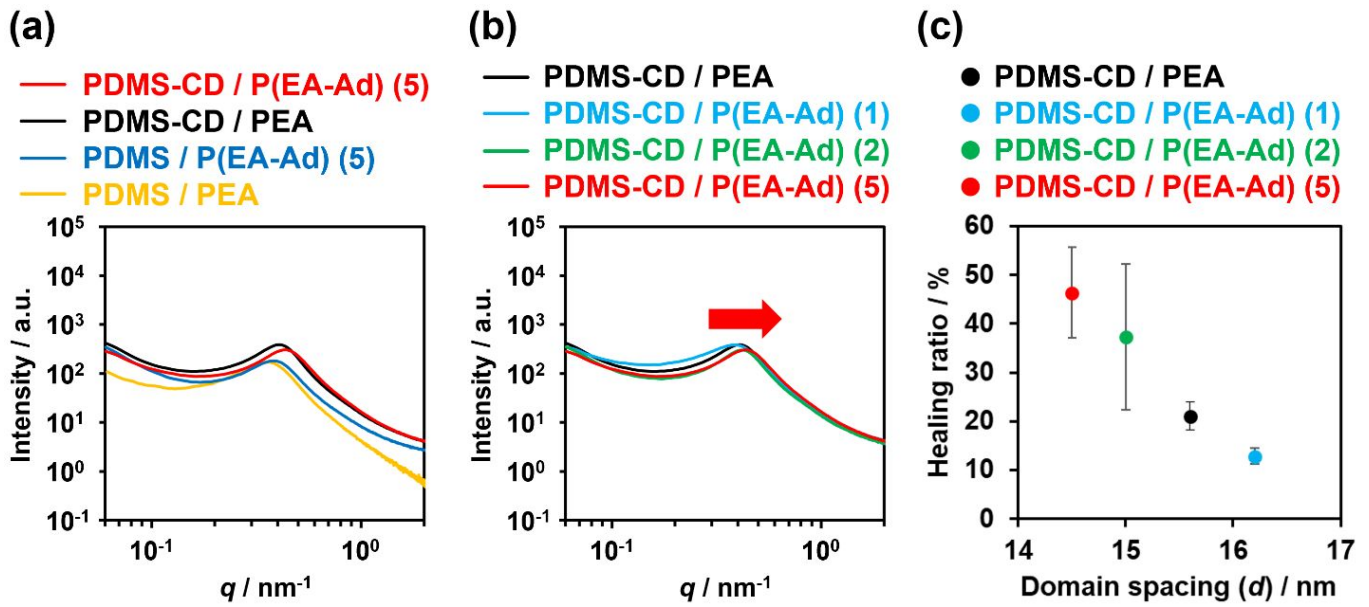

Figure 6. SAXS profiles of **(a)** PDMS-CD/P(EA-Ad) (5), PDMS-CD/PEA, PDMS/P(EA-Ad) (5), and PDMS/PEA. **(b)** SAXS profiles and **(c)** plots of the domain spacing (*d*) and healing ratio of PDMS-CD/PEA and PDMS-CD/P(EA-Ad) (*x*) (*x* = 1, 2, and 5).

Ad) (*x*) with reversible cross-links can be re-adhered after cutting. These samples have the high mixability of PDMS and acrylate polymers. PDMS-CD/P(EA-Ad) (*x*) show greater stretchability than elastomers without βCD and Ad. When the equivalents of βCD and Ad were the same, they show lower healing efficiency due to the unintended formation of interlocked structures with movable cross-links. Conversely, excess Ad units suppress the formation of movable cross-links and aid in the reformation of reversible cross-links to achieve effective molecular adhesion. The stress relaxation tests support that an excess amount of Ad units improve the reformation and exchange of reversible cross-links. A structural study using SAXS reveals that many Ad units also improve the mixability of PDMS and acrylate polymers to effectively reform reversible cross-links and increase the healing efficiency. These findings provide insight into a design strategy for improving the mixability and self-healing properties of organic–inorganic materials to extend their lifetimes, thereby extending the applicability of PDMS-based composites. We believe that these design strategies are applied to the filler–composite interface, fiber-reinforced plastic, and stimuli-responsive adhesion.

Table 2. Domain spacing (*d*) values of the phase-separated structures in PDMS-CD/P(EA-Ad) (*x*) (*x* = 1, 2, and 5), PDMS-CD/PEA, PDMS/P(EA-Ad) (5), and PDMS/PEA.

	d / nm
PDMS-CD/P(EA-Ad) (1)	16.2
PDMS-CD/P(EA-Ad) (2)	15.0
PDMS-CD/P(EA-Ad) (5)	14.5
PDMS-CD/PEA	15.6
PDMS/P(EA-Ad) (5)	16.4
PDMS/PEA	17.9

Conflicts of interest

There are no conflicts to declare.

Data availability

The data supporting this article have been included as part of the Supplementary Information.

Acknowledgements

This research was funded by Scientific Research on Innovative Areas JP19H05714 and JP19H05721 from the MEXT of Japan, JST; the Core Research for Evolutional Science and Technology (CREST) program JPMJCR22L4; the COI-NEXT program JPMJPF2218; the JSPS Core-to-Core Program JPJSCCA20220006; the Asahi Glass Foundation; the Yazaki Memorial Foundation for Science (Y.T.); International Polyurethane Technology Foundation; Toyota Riken Scholar Program (R.I.); the Iketani Science and Technology Foundation, 0351026-A and 0361034-A (R.I. and K.Y.); and the Suzuki Foundation (K.Y.). The authors would like to thank Dr Keiichi Osaka, Dr Noboru Ohta, and Yuka Ikemoto at the Japan Synchrotron Radiation Research Institute (JASRI) for the synchrotron radiation measurements. Synchrotron radiation experiments were performed at BL19B2 of SPring-8 with the approval of JASRI (Proposal Nos. 2022B0578). We thank Dr. Naoya Inazumi and the Analytical Instrumental Facility, Graduate School of Science, Osaka

University, for supporting the NMR measurements and FT-IR spectroscopy.

References

1 L. Yu, K. Dean and L. Li, *Prog. Polym. Sci.*, 2006, **31**, 576–602.
2 D. Myung, D. Waters, M. Wiseman, P.-E. Duhamel, J. Noolandi, C. N. Ta and C. W. Frank, *Polym. Adv. Technol.*, 2008, **19**, 647–657.
3 K. Katsumata, T. Saito, F. Yu, N. Nakamura and Y. Inoue, *Polym. J.*, 2011, **43**, 484–492.
4 T. Uemura, T. Kaseda, Y. Sasaki, M. Inukai, T. Toriyama, A. Takahara, H. Jinnai and S. Kitagawa, *Nat. Commun.*, 2015, **6**, 7473.
5 Q. V. Bach, C. M. Vu, H. T. Vu, T. Hoang, T. V. Dieu and D. D. Nguyen, *Polym. J.*, 2020, **52**, 345–357.
6 H. N. Apostoleris, M. Chiesa and M. Stefancich, *J. Mater. Chem. C.*, 2015, **3**, 1371–1377.
7 T. M. Reidy, D. Luo, P. Rana, B. Huegel and X. Cheng, *J. Micromech. Microeng.*, 2019, **29**, 015014.
8 J. C. Lötters, W. Olthuis, P. H. Veltink and P. Bergveld, *J. Micromech. Microeng.*, 1997, **7**, 145–147.
9 S. C. B. Mannsfeld, B. C. K. Tee, R. M. Stoltenberg, C. V. H. H. Chen, S. Barman, B. V. O. Muir, A. N. Sokolov, C. Reese and Z. Bao, *Nat. Mater.*, 2010, **9**, 859–864.
10 M. Ionescu, B. Winton, D. Wexler, R. Siegele, A. Deslantes, E. Stelcer, A. Atanacio and D. D. Cohen, *Nucl. Instrum. Methods Phys. Res. B*, 2012, **273**, 161–163.
11 I. Miranda, A. Souza, P. Sousa, J. Ribeiro, E. M. S. Castanheira, R. Lima and G. Minas, *J. Funct. Biomater.*, 2022, **13**, 2.
12 R. Iqbal, B. Majhy and A. K. Sen, *ACS Appl. Mater. Interfaces*, 2017, **9**, 31170–31180.
13 T. S. Radhakrishnan, *J. Appl. Polym. Sci.*, 2005, **99**, 2679–2686.
14 U. Eduok, O. Faye and J. Szpunar, *Prog. Org. Coat.*, 2017, **111**, 124–163.
15 X. Zhang, H. Zhang, D. Li, H. Xu, Y. Huang, Y. Liu, D. Wu and J. Sun, *Compos. B*, 2021, **224**, 109207.
16 M. K. Kwak, H. E. Jeong and K. Y. Suh, *Adv. Mater.*, 2011, **23**, 3949–3953.
17 H. Zhou, H. Wang, H. Niu, A. Gestos, X. Wang and T. Lin, *Adv. Mater.*, 2012, **24**, 2409–2412.
18 A. J. T. Teo, A. Mishra, I. Park, Y. J. Kim, W. T. Park and Y. J. Yoon, *ACS Biomater. Sci. Eng.*, 2016, **2**, 454–472.
19 S. Kim, S. H. Ye, A. Adamo, R. A. Orizondo, J. Jo, S. K. Cho and W. R. Wagner, *J. Mater. Chem. B*, 2020, **8**, 8305–8314.
20 N. Lu, C. Lu, S. Yang and J. Rogers, *Adv. Funct. Mater.*, 2012, **22**, 4044–4050.
21 T. G. Yun, M. Park, D. H. Kim, D. Kim, J. Y. Cheong, J. G. Bae, S. M. Han and I. D. Kim, *ACS Nano*, 2019, **13**, 3141–3150.
22 J. Brandup, E. H. Immergut, E. A. Grulke, *Polymer Handbook*, John Wiley & Sons, Hoboken, New Jersey, 4th edn, 1999, ch. 7, pp. 675–714.
23 J. E. Mark, *Polymer Data Handbook*, Oxford University Press, Oxford, 1999, pp. 414.
24 D. W. V. Krevelen, K. T. Nijenhuis, *Properties of Polymers*, Elsevier, Amsterdam, The Netherlands, 4th edn, 2009, ch. 7, pp. 189–227.
25 T. D. Jones, J. S. Schulze, C. W. Macosko and T. P. Lodge, *Macromolecules*, 2003, **36**, 7212–7219.
26 W. Gong, K. Zeng, L. Wang and S. Zheng, *Polymer*, 2008, **49**, 3318–3326.
27 J. Rovere, C. A. Correa, V. G. Grassi and M. F. D. Pizzol, *J. Mater. Sci.*, 2008, **43**, 952–959.
28 J. Bonnet, V. Bounor-Legaré, P. Alcouffe and P. Cassagnau, *Mater. Chem. Phys.*, 2012, **136**, 954–962.
29 T. P. T. Dao, F. Fernandes, E. Ibarboure, K. Ferji, M. Prieto, O. Sandre and J. F. Le Meins, *Soft Matter*, 2017, **13**, 627–637.
30 S. S. Banerjee, S. Banerjee, S. Wießner, A. Janke, G. Heinrich and A. Das, *Macromol. Mater. Eng.*, 2021, **306**, 2100380.
31 X. W. He, J. M. Widmaier, J. E. Herzt and G. C. Meyer, *Polymer*, 1992, **33**, 866–871.
32 S. Murayama, S.-I. Kuroda and Z. Osawa, *Polymer*, 1993, **34**, 2845–2852.
33 L. H. Sperling and V. Mishra, *Polym. Adv. Technol.*, 1996, **7**, 197–208.
34 A. J. Silvaroli, T. R. Heyl, Z. Qiang, J. M. Beebe, D. Ahn, S. Mangold, K. R. Shull and M. Wang, *ACS Appl. Mater. Interfaces*, 2020, **12**, 44125–44136.
35 R. M. Kappel, A. J. H. Klunder and G. J. M. Pruijn, *Eur. J. Plast. Surg.*, 2014, **37**, 123–128.
36 T. Miao, S. L. Fenn, P. N. Charron and R. A. Oldinski, *Biomacromolecules*, 2015, **16**, 3740–3750.
37 F. Wu, L. Chen, Y. Wang and B. Fei, *J. Mater. Sci.*, 2019, **54**, 12131–12144.
38 D. Zhao, Z. Zhang, J. Zhao, K. Liu, Y. Liu, G. Li, X. Zhang, R. Bai, X. Yang and X. Yan, *Angew. Chem. Int. Ed.*, 2021, **60**, 16224–16229.
39 Y. Liu, J. Jian, Y. Xie, S. Gao, D. Zhang, H. Shi, Y. Xu, C. Lai, C. Wang and F. Chu, *J. Mater. Sci.*, 2022, **57**, 12138–12146.
40 G. Lee, H. Seo, D. Kim, S. Shin and K. Kwon, *RSC Adv.*, 2023, **13**, 1672–1683.
41 R. Ikura, J. Park, M. Osaki, H. Yamaguchi, A. Harada and Y. Takashima, *Macromolecules*, 2019, **52**, 6953–6962.
42 P. Cordier, F. Tournilhac, C. Soulié-Ziakovic and L. Leibler, *Nature*, 2008, **451**, 977–980.
43 S. Burattini, H. M. Colquhoun, J. D. Fox, D. Friedmann, B. W. Greenland, P. J. F. Harris, W. Hayes, M. E. MacKay and S. J. Rowan, *Chem. Commun.*, 2009, 6717–6719.
44 E. M. Pouget, P. H. H. Bomans, J. A. C. M. Goos, P. M. Frederik, G. De With and N. A. J. M. Sommerdijk, *Science*, 2009, **323**, 1455–1458.
45 J. Canadell, H. Goossens and B. Klumperman, *Macromolecules*, 2011, **44**, 2536–2541.
46 K. Imato, M. Nishihara, T. Kanehara, Y. Amamoto, A. Takahara and H. Otsuka, *Angew. Chem. Int. Ed.*, 2012, **51**, 1138–1142.
47 M. Burnworth, L. Tang, J. R. Kumpfer, A. J. Duncan, F. L. Beyer, G. L. Fiore, S. J. Rowan and C. Weder, *Nature*, 2011, **472**, 334–337.
48 F. Herbst, S. Seiffert and W. H. Binder, *Polym. Chem.*, 2012, **3**, 3084–3092.
49 M. Zhang, D. Xu, X. Yan, J. Chen, S. Dong, B. Zheng and F. Huang, *Angew. Chem. Int. Ed.*, 2012, **51**, 7011–7015.
50 T. L. Sun, T. Kurokawa, S. Kuroda, A. Bin Ihsan, T. Akasaki, K. Sato, M. A. Haque, T. Nakajima and J. P. Gong, *Nat. Mater.*, 2013, **12**, 932–937.
51 S. Chen, N. Mahmood, M. Beiner and W. H. Binder, *Angew. Chem.* 2015, **127**, 10326–10330.
52 Y. Cao, T. G. Morrissey, E. Acome, S. I. Allec, B. M. Wong, C. Keplinger and C. Wang, *Adv. Mater.*, 2017, **29**, 1605099.
53 T. Nakajima, *Polym. J.*, 2017, **49**, 477–485.
54 R. Tamate, *Polym. J.*, 2021, **53**, 789–798.
55 A. N. Au-Duong, Y. C. Hsu, M. Malintoi, A. N. Ubaidillah, Y. T. Li, J. Y. Lai and Y. C. Chiu, *Polym. J.*, 2022, **54**, 305–312.
56 M. Nakahata, Y. Takashima, H. Yamaguchi and A. Harada, *Nat. Commun.*, 2011, **2**, 511.
57 T. Kakuta, Y. Takashima, M. Nakahata, M. Otsubo, H. Yamaguchi and A. Harada, *Adv. Mater.*, 2013, **25**, 2849–2853.
58 S. Nomimura, M. Osaki, J. Park, R. Ikura, Y. Takashima, H. Yamaguchi and A. Harada, *Macromolecules*, 2019, **52**, 2659–2668.
59 D. Yoshida, J. Park, R. Ikura, N. Yamashita, H. Yamaguchi and Y. Takashima, *Chem. Lett.*, 2023, **52**, 93–96.
60 D. Yoshida, J. Park, N. Yamashita, R. Ikura, N. Kato, M. Kamei, K. Ogura, M. Igarashi, H. Nakagawa and Y. Takashima, *Polym. Chem.*, 2023, **14**, 3277–3285.

61 N. Yamashita, K. Yamaoka, R. Ikura, D. Yoshida, J. Park, N. Kato, M. Kamei, K. Ogura, M. Igarashi, H. Nakagawa and Y. Takashima, *Soft Matter*, 2023, **19**, 9074–9081.
62 R. Ikura, K. Kajimoto, J. Park, S. Murayama, Y. Fujiwara, M. Osaki, T. Suzuki, H. Shirakawa, Y. Kitamura, H. Takahashi, Y. Ohashi, S. Obata, A. Harada, Y. Ikemoto, Y. Nishina, Y. Uetsuji, G. Matsuba and Y. Takashima, *ACS Polymers Au*, 2023, **3**, 394–405.

OSAKA UNIVERSITY
Department of Macromolecular Science
Graduate School of Science

Data Availability Statement

The data supporting the article have been included as part of the Supplementary Information.

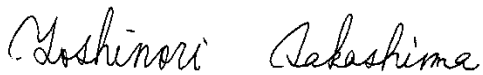

Yoshinori Takashima

Professor Dr. Yoshinori Takashima
1-1 Machikaneyama-cho, Toyonaka,
Osaka 560-0043, Japan
Phone: +81-6-6850-5447, Fax: +81-6-6850-5447
e-mail: takasima@chem.sci.osaka-u.ac.jp